Current Cardiovascular Imaging Reports (2019) 12: 18
https://doi.org/10.1007/s12410-019-9489-1

CARDIAC MAGNETIC RESONANCE (E NAGEL AND V PUNTMANN, SECTION EDITORS)

Cardiac MRI: a Promising Diagnostic Tool to Detect Cancer Therapeutics–Related Cardiac Dysfunction

Jasmin D. Haslbauer[1] · Sarah Lindner[2] · Gesine Bug[2] · Eike Nagel[1] · Valentina O. Puntmann[1]

Published online: 3 April 2019

Abstract

Purpose of Review Recent advances in oncological research have led to a major improvement of mortality amongst cancer patients. However, survivors are at an increased risk to develop cancer therapeutics–related cardiac dysfunction (CTRCD). The management of CTRCD may pose a challenge due to its heterogeneous clinical presentation. This warrants the need for a multi-modality diagnostic tool to objectively acquire prognostic information for timely commencement of cardio-protective treatment. Cardiac magnetic resonance (CMR) imaging offers considerable potential due to its non-invasive, reproducible protocol. Moreover, biomarkers such as T1 and T2 mapping allow discrimination between oedematous and fibrotic myocardium, providing an invaluable diagnostic algorithm to track the temporal evolution of CTRCD.

Recent Findings In this review, we appraise current evidence for the role of CMR in the management of CTRCD, placing emphasis on ventricular function, strain, late gadolinium enhancement and parametric mapping.

Summary We recommend a central role for CMR in the interdisciplinary management of CTRCD.

Keywords Cardio-oncology · Cardiac magnetic resonance · Cancer therapeutics · Cardiotoxicity · Anthracyclines

Abbreviations

2/3DE	2D/3D echocardiography
AI	Artificial intelligence
ATP	Adenosine triphosphate
CMR	Cardiac magnetic resonance
CTLA-4	Cytotoxic T lymphocyte–associated Protein 4
CTRCD	Cancer therapeutics–related cardiac dysfunction
CV	Cardiovascular
ECV	Extracellular volume
EDV	End-diastolic volume
ESV	End-systolic volume
EMB	Endomyocardial biopsy
ESC	European Society of Cardiology
GCS	Global circumferential strain
GLS	Global longitudinal strain
HF	Heart failure
hs-troponinT	High-sensitive troponin T
LGE	Late gadolinium enhancement
LV	Left ventricular
LVEF	Left ventricular ejection fraction
NT-proBNP	N-terminal pro-brain natriuretic peptide
NSCLC	Non-small cell lung cancer
PD1	Programmed cell death protein 1
PDL1	Programmed cell death protein ligand 1
PWV	Pulse wave velocity
QOL	Quality of life

This article is part of the Topical Collection on *Cardiac Magnetic Resonance*

✉ Valentina O. Puntmann
vppapers@icloud.com

Jasmin D. Haslbauer
JasminDionne.Haslbauer@kgu.de

Sarah Lindner
Sarah.Lindner@kgu.de

Gesine Bug
Gesine.Bug@kgu.de

[1] Institute of Experimental and Translational Cardiovascular Imaging, DZHK Centre for Cardiovascular Imaging, Goethe University Hospital Frankfurt, Frankfurt, Germany

[2] Department of Haematology and Oncology, Goethe University Hospital Frankfurt, Frankfurt, Germany

ROS	Reactive oxygen species
RVEF	Right ventricular ejection fraction
SSFP	Steady-state free precession
TKI	Tyrosine kinase inhibitors

Background: Why CMR Is a Promising Diagnostic Tool to Manage Cancer Therapeutics–Related Cardiac Dysfunction

In recent years, advances in antineoplastic therapy schemes have resulted in a decrease of mortality rates and the emergence of personalised medicine in oncology [1, 2]. However, the management of cardiotoxic adverse effects such as cancer therapeutics–related cardiac dysfunction (CTRCD) remains a challenge in the post-therapeutic phase [3–5]. Consequently, modern cardio-oncological research has prioritised on optimising detection and monitoring of cardiotoxicity to ensure timely commencement of cardio-protective measures, thus aiming to improve quality of life and survival amongst cancer patients [6•, 7].

The pharmacology and underlying pathophysiological mechanisms of CTRCD are complex; Table 1 offers an overview of potentially cardiotoxic agents. Two main types of myocardial damage are widely discussed in the literature: type 1 (anthracycline-mediated; typically irreversible) and type 2 (Her2/Neu inhibitor-mediated; typically reversible) [8, 14]. Anthracyclines such as daunorubicin and epirubicin are known to inhibit both DNA replication and RNA transcription and facilitate the formation of reactive oxygen species (ROS), causing increased oxidative stress leading to myocyte apoptosis and remodelling [8]. They also directly cause membrane damage due to lipid oxidation and inhibit topoisomerase II, thus halting tumour cell growth [15]. Histopathological findings suggest the development of oedema, vacuolisation and myocardial inflammation which precede diffuse interstitial fibrosis [16, 17]. Clinical manifestations observed include typical sequential development starting with myocardial ischaemia and/or myopericarditis which can eventually lead to overt heart failure [3] (Fig. 1). These changes are dose-dependent and irreversible and can develop years after receiving therapy. The pathophysiology of Her2/Neu inhibitor–mediated CTRCD, on the other hand, is more poorly understood. It is postulated that trastuzumab administration leads to ATP depletion in the myocardiocytes through the neuregulin-1/ErbB2 pathway, thus causing contractile dysfunction [11, 18, 19]. Conversely to type 1 cardiotoxicity, damage is dosage-independent and typically reversible, although some irreversible cases have been reported [20–22]. Table 2 provides an overview of current chemotherapy regimens containing anthracyclines and/or Her2/Neu inhibitors.

Recent advances in oncological drug development have led to the approval of a plethora of potentially cardiotoxic drugs. Reports on cardiovascular adverse

Table 1 Overview of major cancer therapeutics classes and underlying pathophysiological changes in myocardial dysfunction. This table offers an updated overview of the main antineoplastic substances associated with cardiotoxicity, as well as a brief description of their pathophysiology. Most studies focus on anthracyclines and Her2/Neu inhibitor–associated CTRCD. *5-FU*, 5 fluorouracil; *MTX*, methotrexate

Cancer therapeutics class	Agents
Chemotherapy: Formation of ROS causes increased oxidative stress, leading to myocyte apoptosis and remodelling. Clinically, this can manifest as ventricular dysfunction, CHF, myocardial ischaemia and myopericarditis. These changes are dose-dependent and irreversible.	
Anthracyclines	Doxorubicin, daunorubicin, epirubicin, idarubicin, mitoxantrone [8]
Alkylating agents	Cyclophosphamide, ifosfamide, cisplatin, carmustine, busulfan, chlormethine, mitomycin [9]
Antimetabolites	5-FU, cytarabine, MTX, fludarabine [10]
Antimicrotubule agents	Docetaxel, paclitaxel, etoposide, teniposide, vincristine, vinblastine [10]
Monoclonal antibodies: These lead to different pathophysiological changes depending on drug class. Mechanisms include endogenous modulation of oxidative stress, inhibition of cellular repair mechanisms and myocyte contractile dysfunction. Clinically, this can manifest as CHF, myocardial ischaemia and myopericarditis. These changes are not dose-dependent and are reversible.	
Her2/Neu inhibitors	Trastuzumab, pertuzumab [11]
Tyrosine kinase inhibitors (TKIs)	Imatinib, dasatinib, nilotinib, ponatinib, sunitinib, sorafenib, pazopanib, erlotinib, lapatinib, lenvatinib, vandetanib [12]
Checkpoint inhibitors	Ipilimumab, nivolumab, pembrolizumab [13]
Miscellaneous agents	
Bleomycin, interferon, interleukin 2, tretinoin, proteasome inhibitors (bortezomib, carfilzomib) [10]	
Radiation therapy: ROS formation leads to dsDNA strand breaks and oxidative stress. Secondary inflammation and apoptotic changes lead to fibrosis.	

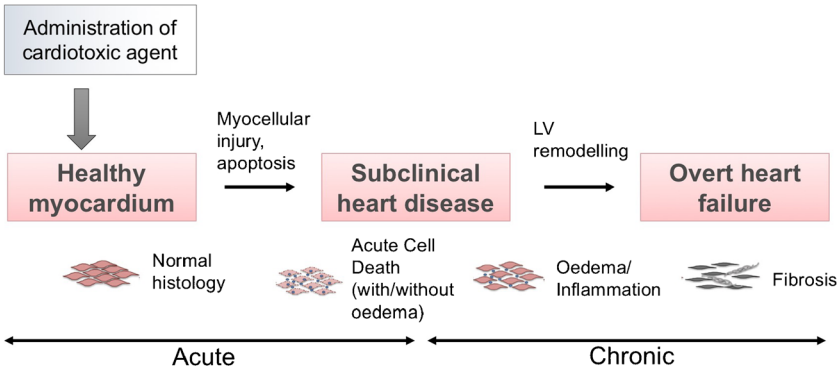

Fig. 1 Temporal evolution of CTRCD from subclinical stage to overt heart failure. This flow chart depicts the pathophysiological changes and their temporal evolution in the myocardium when a potentially cardiotoxic agent is administered. Subclinical heart disease varies in severity, depending on the extent of myocellular injury and apoptosis. Areas of the myocardium with high inflammatory infiltrate eventually undergo fibrotic remodelling which can lead to overt heart failure. LV = left ventricular. Adapted from Manrique et al. (2017) [3], with permission

events caused by tyrosine kinase inhibitors (TKIs) like imatinib and dasatinib or immune checkpoint inhibitors like ipilimumab show high heterogeneity in clinical presentation, and the underlying pathophysiology is not fully understood [12, 62, 63]. This further emphasises the necessity for further research using novel diagnostic tools to elucidate the mechanisms and monitor potential adverse effects.

In view of the above discussed, methods for early detection of subclinical cardiac injury are essential to identify patients who would potentially benefit from cardio-protective therapy measures which would preserve cardiac function, thus halting remodelling. Echocardiography has been overwhelmingly used for this purpose due to its wide availability and lack of radiation. An ESC position paper published in 2016 recommends baseline echocardiographic assessment of LV function before initiation of potentially cardiotoxic cancer treatment in all patients, irrespective of clinical history, and for follow-up screening [6•]. However, major limitations include high inter-observer and inter-vendor reproducibility and varying acoustic window quality [6•, 64]. Image quality in 2D-echocardiography (2DE) is dependent on acoustic windows which are determined by effective endocardial border definition and on geometric assumptions—these may not apply to patients with dilated or remodelled ventricles [65]. Recent results with 3D-echocardiography (3DE) with automated contouring have therefore been introduced with better reproducibility [66]; however, the problems of acoustic windows remain [67–69].

Furthermore, although the use of serological biomarkers such as troponin and NT-proBNP may show promise to detect cardiotoxicity in its subclinical stage, there is currently no standardised scheme for their application, largely due to uncertainties in measurement threshold and timing, as well as discrepancies between assays [70–73]. Both troponin and NT-proBNP are not specific for CTRCD and this may pose a problem for patients with cardiovascular comorbidities. In addition, subtle changes in troponin may be difficult to interpret without morphologic correlates due to growing evidence suggesting that increases in its serum concentration may be more sensitive than histologic analysis [74].

More recent work has led to the incorporation of cardiovascular magnetic resonance (CMR) into the expert consensus of multi-modality diagnostics of cardiotoxicity [64]. CMR holds the gold-standard assessment for LV function and volume assessment, is radiation-free, highly reproducible and features myocardial strain assessment, characterisation of early microstructural and microvascular changes and assessment of pericardial disease [64]. Furthermore, tissue characterisation by T1 and T2 mapping, a feature unique to CMR, allows non-invasive discrimination between oedematous and fibrotic myocardium, providing a reproducible diagnostic algorithm to track the temporal evolution of subclinical and late stages in CTRCD patients [75•](Fig. 2). Moreover, measuring T1 maps pre- and post-contrast at sufficient contrast equilibrium enables acquisition of ECV (extracellular volume), a measure elevated in fibrosis or infiltration. In this review, we summarise existing data on the utility of CMR to detect CTRCD, focussing on recent developments in (a) quantification of ventricular function, (b) myocardial strain, (c) late gadolinium enhancement (LGE) and (d) parametric mapping. For quick reference, Table 3 lists major clinical publications featuring CTRCD conducted using CMR from 2013 to 2018.

Cardiac MRI Imaging Protocol: Diagnostic Utility of CMR to Detect CTRCD

Ventricular Function

An expert committee led by Seidman et al. initially defined CTRCD as one or more of the following: [1], LVEF reduction (either globally reduced or specifically affecting the

Table 2 Systemically administered anthracycline and Her2/Neu-containing regimens. A complete list of all antineoplastic therapy regimens containing either systemic administration of anthracyclines and/or Her2/NEU inhibitors. Abbreviations of individual schemes are fully elucidated in the respective column. Italicize = cardiotoxic anthracycline, Her2/NEU inhibitor. SCLC = small cell lung cancer, ALL = acute lymphoblastic leukaemia, AML = acute myeloblastic leukaemia, MM = multiple myeloma, HL = Hodgkin lymphoma, NHL = non-Hodgkin lymphoma, ART = antiretroviral therapy, LOH = loss of heterozygosity

Tumour entity	Regimen (+abbreviation)		Indication
Gynaecological			
Breast, Her2/Neu+	AC-P + Trast (+Pert)	*Doxorubicin*, cyclophosphamide, paclitaxel, *trastuzumab*, (*pertuzumab*)	(Neo)-adjuvant chemotherapy, Her2/Neu+ localised/inoperable locally advanced disease (stages I, IIA, IIB or IIIA (T3N + M0)) [23, 24]
	AC-T + Trast (+Pert)	*Doxorubicin*, cyclophosphamide, docetaxel, *trastuzumab*, (*pertuzumab*)	
	TCH (+Pert)	Docetaxel, carboplatin, *trastuzumab*, (*pertuzumab*)	Adjuvant chemotherapy, Her2/Neu+ localised/inoperable locally advanced disease (stages I, IIA, IIB or IIIA (T3N + M0)) with contraindications against receiving anthracyclines or Her2/Neu+ metastatic disease [23]
	Pert/Trast - D	*Pertuzumab*, *trastuzumab*, docetaxel	Her2/Neu+ metastatic disease
Breast, Her2/Neu−	TAC	Docetaxel, *doxorubicin*, cyclophosphamide	Adjuvant chemotherapy, Her2/Neu− localised/inoperable locally advanced disease (stages I, IIA, IIB or IIIA (T3N + M0)0029 [25, 26]
	AC/EC (−T) (−P)	*Doxorubicin/epirubicin*, cyclophosphamide (+ paclitaxel/docetaxel)	Adjuvant chemotherapy, Her2/Neu− localised/inoperable locally advanced disease (stages I, IIA, IIB or IIIA (T3N + M0)) or recurrent/metastatic disease [27–35]
	FAC	5-FU, *doxorubicin*, cyclophosphamide	
	FEC (−T) (−P)	Cyclophosphamide, *epirubicin*, 5-FU (+ docetaxel or paclitaxel)	
	EC	*Epirubicin*, cyclophosphamide	
	EP/AP	*Epirubicin/doxorubicin*, paclitaxel	
	ET/AT	*Epirubicin/doxorubicin*, docetaxel	
Breast, Her2/Neu− or +	M(C)	*Liposomal doxorubicin* (Myocet®) + cyclophosphamide	Recurrent/metastatic disease [36]
Ovary	*Pegylated doxorubicin* (Caelyx®) (+ trabectedin)		2nd line refractory disease [37]
Endometrium	Platin + epirubicin/doxorubicin		2nd line for advanced, recurrent, metastatic disease [38]
Gastrointestinal			
Stomach	EOX	*Epirubicin*, oxaliplatin, capecitabine	Recurrent/metastatic disease [39]
	5-FU, cisplatin, *trastuzumab*		Her2+ metastatic gastric or adenocarcinoma of the GEJ (gastroesophageal junction) [40]
Head, neck, respiratory tract			
SCLC	CAV/CEV	Cyclophosphamide, *doxorubicin/epirubicin*, vincristine	2nd line in limited/extensive disease [41]
Thyroid	*Doxorubicin* (in combination with cisplatin)		Poorly differentiated/anaplastic thyroid cancer; metastatic disease [42]
Squamous upper respiratory tract	MVAC	Methotrexate, vinblastine, *doxorubicin*, cisplatin	Recurrent/metastatic disease [43]
Haematological			
ALL	Vincristine, corticosteroids, and anthracycline (*daunorubicin*, *doxorubicin*, *rubidazone*, *idarubicin*), with or without cyclophosphamide or cytarabine		Induction therapy according to paediatric BFM (widespread in Europe) [44]
	Hyper-CVAD	Cyclophosphamide, vincristine, *doxorubicin*, dexamethasone	8 alternating intensive cycles identical for induction and consolidation (preferentially used in the USA) [44]
AML	(*Liposomal*) *daunorubicin*, cytarabine		3 + 7 induction regimen [45]
	Idarubicin, cytarabine		Induction and consolidation [45]
MM	PAD	Bortezomib, *doxorubicin*, low-dose dexamethasone	Relapsed/refractory disease [46]

Table 2 (continued)

Tumour entity	Regimen (+abbreviation)		Indication
HL	ABVD	*Doxorubicin*, bleomycin, vinblastine, dacarbazine	Newly diagnosed disease, stages I and II [47]
	BEACOPP	Bleomycin, etoposide, *doxorubicin*, cyclophosphamide, vincristine (oncovin), procarbazine, prednisolone	Newly diagnosed disease, stages I and II with risk factors and/or > stage IIB (+ radiation) [48]
NHL	(R)- CHOP	(Rituximab), cyclophosphamide, *doxorubicin*, vincristine (oncovin), prednisolone	Newly diagnosed/refractory disease [49]
	(R)- CHEOP	(Rituximab), cyclophosphamide, etoposide, *doxorubicin*, vincristine (oncovin), prednisolone	Newly diagnosed/refractory disease [50]
	Pixantrone	Modified *mitoxantrone*	Relapsed/refractory diffuse large B cell lymphoma (DLBCL) [51]
Kaposi sarcoma	(ART) + ABV	Antiretroviral therapy, vincristine, bleomycin, (*liposomal*) *doxorubicin/daunorubicin*	Severe/symptomatic disease – immediate initiation of ART in combination with systemic chemotherapy [52]
Urological			
Bladder	MVAC	Methotrexate, vinblastine, *doxorubicin*, cisplatin	Neoadjuvant therapy of localised muscle-invasive disease or 2nd line in advanced disease [53, 54]
Interstitial			
Soft tissue sarcomas	*Doxorubicin* (+ Ifosfamide)		Newly diagnosed/refractory disease [55]
	Doxorubicin + olaratumab		Newly diagnosed/refractory disease [56]
Paediatric			
Ewing sarcoma	VDC	Vincristine, *doxorubicin*, cyclophosphamide	Newly diagnosed disease [57]
Osteosarcoma	*Doxorubicin*, cisplatin, methotrexate (± mifamurtide)		1st line neoadjuvant therapy [58]
Nephroblastoma (Wilms tumour)	Vincristine, dactinomycin, *doxorubicin*		Adjuvant post-nephrectomy: stages I and II favourable histology with LOH 1p and 16q or stages III and IV favourable histology without LOH 1p and 16q [59]
	Vincristine, dactinomycin, *doxorubicin*, cyclophosphamide, etoposide		Adjuvant post-nephrectomy: stages III and IV favourable histology with LOH 1p and 16q [59]
Neuroblastoma	Cyclophosphamide, *doxorubicin*/cisplatin, teniposide		Unresectable low risk disease / neoadjuvant therapy [60]
	Topotecan, vincristine, *doxorubicin*		Stage 4 high-risk disease after failing to achieve metastatic response to 1st line therapy [61]

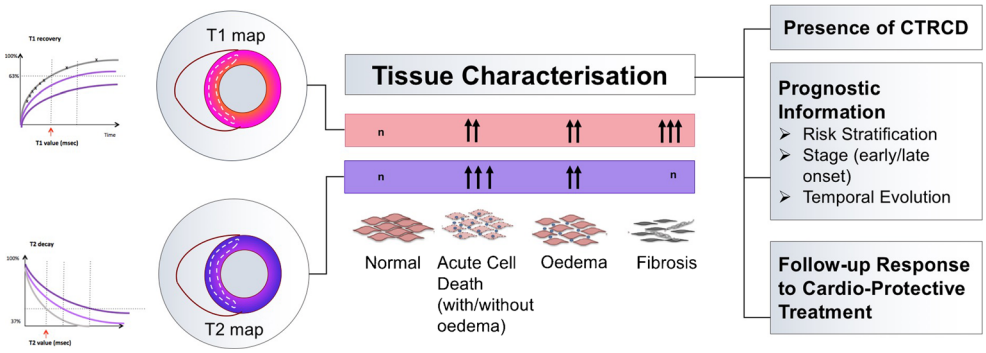

Fig. 2 Tissue characterisation by T1 and T2 mapping provides novel insights into prognosis and follow-up of CTRCD. T1 and T2 parametric mapping are novel CMR parameters that allow myocardial tissue characterisation. They have been previously used in a wide aetiology of cardiomyopathies, as well as in patients with CTRCD. Elevated T1 values imply fibrotic remodelling, while elevated T2 values measure the amount of oedematous content in the myocardium. T1 in conjunction with T2 mapping can be used as a novel diagnostic algorithm for risk stratification, temporal evolution and follow-up for patients with CTRCD

Table 3 Overview of clinical studies using CMR as a diagnostic tool for the detection of CTRCD

Author, year	Method	Cancer	*n*	Treatment	Imaging timing	Main findings
Gong et al. (2018) [76]	Strain using FT-CMR (GCS, GLS, GLSR-E, GCSR-E, GRSR-E), LVEF	Breast	41	Trastuzumab	Baseline, 6, 12 and 18 months after treatment initiation	Significant decrease GLS, GLS and LVEF after 6 months, followed by a recovery by 18 months. Diastolic strain (GLSR-E and GCSR-E) showed no significant change over 18 months. Systolic strains are more likely useful than diastolic strain for monitoring subclinical trastuzumab-related myocardial dysfunction.
Kimball et al. (2018) [77]	T1 mapping, LVEF	Breast	46	Anthracyclines and trastuzumab	5 ± 1 year post--chemotherapy	Follow-up imaging of the same cohort from Grover et al. (2013) [78] (see below) investigating late-onset effects. Statistically but not clinically significant decrease in LVEF was observed from baseline to 5 years. T1 values remained within normal limits 5 years post-therapy and showed no correlation with LV or RVEF, implying minimal long-term cardiac toxicity.
Ferreira de Souza et al. (2018) [79]	LVEF, T2-weighted signal intensity for myocardial oedema, ECV, LV mass, τic (intracellular water lifetime), LGE	Breast	27	Anthracyclines	Baseline and 3 times post-therapy (351–700 days)	At 351 to 700 days post-therapy, a decline in mean LVEF and LV mass was observed. Mean ECV increase, while τic decreased. Myocardial oedema was most extensive at 146–231 days. The decrease in LV mass was postulated to derive from cardiomyocyte atrophy caused by remodelling processes.
Mühlberg et al. (2018) [80]	T1 mapping, T2 mapping, ECV, SSFP cine at 1.5T, LGE	Sarcoma	30	Anthracyclines	Baseline, 48 h after first therapy, upon completion of therapy	9 out of 30 patients developed anthracycline-induced cardiomyopathy 48 h post-treatment; these patients had significantly lower myocardial T1 values compared to before therapy, and also displayed decreased LVEF.
Haslbauer et al. (2018) [75]	T1 mapping, T2 mapping, cardiac function, strain, ischaemia testing, LGE	Multiple	57	Multiple	3 months (early Tx) or > 12 months (late Tx) after treatment initiation	Patients had decreased LVEF and strain, and higher native T1 and T2 than controls. Early Tx group had higher native T1 and T2 compared to late Tx which displayed raised native T1, increased LV-end-systolic volume, reduced LVEF and deformation. This demonstrates that novel biosignatures in CMR detect early cardiac inflammation followed by interstitial remodelling and fibrosis.
Ong et al. (2018) [81]	LVEF, LV strain (GCS, GLS)	Breast	41	Trastuzumab	Baseline, 6, 12, 18 months after treatment initiation	There was a significant reduction of LVEF, as well as GCS and GLS, as well as an increase in LV end-diastolic volume at 6 and 12 months, but not at 18 months.
Jolly et al. (2017) [82]	LV volumes, automated mean mid-wall circumferential strain from cine imaging	Multiple	72	Multiple	Baseline, 3 months post-treatment initiation	At 3 months post-treatment initiation, LVEF decreased compared to baseline. Correlation between strain and CVEF was $r = -0.61$ ($p < 0.0001$).
Barthur et al. (2017) [83]	RV volume	Breast	41	Trastuzumab	Baseline, 6, 12, 18 months post-treatment initiation	Small but significant increases in RV end-diastolic volume at 6 months and significant increase in RV end-systolic volume at 6 and 12 months were observed. These decreases recovered by 18 months. RVEF showed corresponding decreases and recovery.
	GCS, GLS, LVEF	Breast	9	Trastuzumab		

Table 3 (continued)

Author, year	Method	Cancer	*n*	Treatment	Imaging timing	Main findings
Nakano et al. (2016) [84]					Baseline, 3, 6, 12 months after treatment initiation	GCS, GLS and LVEF significantly decreased at 6 months compared to baseline. Similar results were observed for RV circumferential, but not longitudinal strain.
Jordan et al. (2016) [85]	T1 mapping, ECV	Multiple	327	Multiple	2.8 ± 1.3 years after chemotherapy	Native T1 and ECV was elevated pre- (1058 ± 7 ms) and post- (1040 ± 7 ms) receipt of therapy versus healthy individuals. There was no significant difference in T1 and ECV between different chemotherapy regimens or type of cancer. ECV was higher in cancer patients who have received anthracyclines versus pre-treatment or healthy individuals.
Grover et al. (2015) [86]	Cardiac function, PWV of PDA and AA	Breast	41	Anthracyclines and trastuzumab	Baseline, 1, 4 and 14 after treatment initiation	Amongst cancer patients, a decrease in aortic distensibility at AA was measured within 1 and 4 months post-treatment initiation. The PDA only showed a significant reduction at 14 months. Combination therapy with anthracyclines had greater reduction in aortic distensibility.
Grover et al. (2013) [78]	LVEF, RVEF, M:Sk signal intensity ratio	Breast	46	Anthracyclines, taxanes, trastuzumab	Baseline, 1 and 4 months after treatment initiation	Patients showed a persistent functional decline in left and right cardiac functions 1 to 4 months post-treatment initiation. RV function decrease persisted 12 months which correlated with myocardial oedema at 1 and 3 months.
Drafts et al. (2013) [87]	Cardiac function, PWV, LGE	Multiple	53	Anthracyclines	Baseline, 1, 3 and 6 months post-treatment initiation	LV end-systolic volume and PWV increase, as well as LVEF decreased amongst patients at 6 months, correlating with poor quality of life.
Tham et al. (2013) [88]	Cardiac function and mass, T1 and T2 values, ECV	Childhood cancers	30	Anthracyclines	2 years following treatment	Patients displayed normal LVEF but increased ECV, which correlated cumulative dosage. T1 and ECV were identified as early tissue markers of ventricular remodelling, representing diffuse fibrosis
Neilan et al. (2013) [89]	LGE, LV mass	Multiple	91	Anthracyclines	Presentation 88 post-- chemotherapy – follow-up for 27 months	LGE was an uncommon finding. An inverse association between anthracycline dose and indexed left ventricular mass was found. Low LV mass was associated with greater incidence of cardiovascular events.
Ylänen et al. (2013) [90]	Cardiac function, LGE	Childhood cancers	62	Anthracyclines	Long-term survivors (median 7.8 years)	Abnormal LV and RV function were observed amongst 18 and 27% survivors respectively. Both LV/RV end-systolic and end-diastolic values were increased. None of the study patients showed LGE.
Toro-Salazar et al. (2013) [91]	LGE, ECV, Strain, T1	Childhood cancers	46	Anthracyclines	Long-term survivors (2.5–26.9 years)	All subjects did not show LGE. Low average circumferential strain magnitude was corroborated with echocardiography, which yielded similar results. T1 values were lower than that of control subjects.

interventricular septum); [2], clinical symptoms or signs of heart failure (HF); [3], reduction in LVEF from baseline ≤ 5 to < 55% in the presence of signs or symptoms of HF; or [4], a reduction in LVEF ≥ 10 to < 55% without signs or symptoms of HF [92]. Clearly, these cut-off values demand an image modality which has high reproducibility and accuracy of measurements to sufficiently allow detection of small changes which relate to the disease and not the technical noise of the technique (Fig. 2). Unlike echocardiography where quantification is inferred from the 2D dimensional measurements as permitted within acoustic windows of the patients' chest wall, LV chamber quantification using CMR is free from spatial limitations and geometrical assumptions and has excellent image quality in most patients. As such, it allows direct delineation of cardiac structures by endo- and epicardial contouring, providing direct quantification of actual cardiac volumes. Furthermore, standardisation of approaches, which provide a basis of an increasing number of artificial intelligence (AI)–aided quantification algorithms, further strives to reduce the observer interference and an objective derivation of LV parameters. A substantial body of validating evidence for CMR approaches, including superior reproducibility comparing to 2DE or 3DE in patients with heart failure, ventricular hypertrophy and also CTRCD [68, 93, 94], is summarised in recent SCMR expert consensus on CMR measures as endpoints [95•] and is further elucidated in Fig. 3.

The effective differences of diagnostic methods are best exemplified by detection of early subclinical changes of cardiac function. For echocardiography, this remains a challenge owing to poor reproducibility of measurements (intra-observer, inter-observer, for acquisition and post-processing) making detection of subtle, but meaningful early changes difficult [66, 95•]. On the contrary, the robustness of LVEF measurements by CMR was shown to be more feasible, allowing recognition of impaired ventricular function prior to symptomatic disease. Several studies reported detection of changes in patients that have not met diagnostic criteria for cardiotoxicity, as

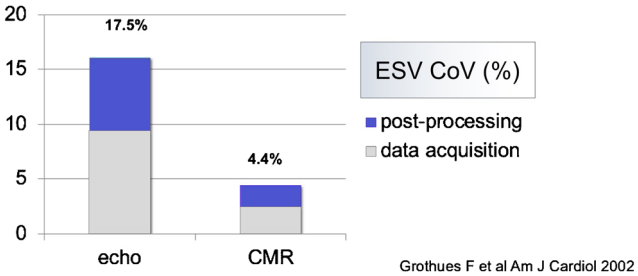

Fig. 3 Comparison of inter-study reproducibility of 2DE vs. CMR measuring end-systolic volume (ESV) in normal subjects and patients with HF or LVEF. Significantly smaller CoV (coefficient of variation) were measured in this study comparing the inter-study reproducibility of different parameters measured by CMR and 2DE. In the case of ESV (end-systolic volume), total CoVs including post-processing and data acquisition were 17.5% for 2DE vs. 4.4% for CMR, showing superior inter-study reproducibility for CMR in this setting

described above, thus precluding early detection of CTRCD [77, 81, 83]. In a study measuring anthracycline-associated cardiomyopathy, 53 breast cancer patients were assessed on LVEF and LV strain using CMR. LVEF in particular decreased within 6 months after low to moderate doses of anthracyclines (58 ± 1 to $53 \pm 1\%$; $p = 0.0002$), thus displaying early development of subclinical abnormalities which were associated with the occurrence of CV events and quality of life (QOL) deterioration in patients with CTRCD [87].

CMR has also shown to be an efficacious method for measuring CTRCD-associated right ventricular dysfunction. A longitudinal investigation led by Barthur et al. screened breast cancer patients receiving trastuzumab using CMR to assess right ventricular function. Results displayed a decrease of both LVEF and RVEF at 6 and 12 months which recovered at 18 months; data is consistent with typical type 2 cardiotoxicity [83].

Furthermore, in a study screening patients with different neoplastic diseases either within 3 months (early toxicity) or more than 12 months (late toxicity) after receiving potentially cardiotoxic treatment, patients in the early group showed a statistically significant decrease in LVEF compared with controls ($55\% \pm 11\%$ vs. $60\% \pm 7\%$; $p < 0.001$); LVEF values were even lower in the late toxicity group ($48\% \pm 12\%$; $p < 0.001$). Data measuring LV mass index, LV-ESV index and LV-EDV index similarly showed significant decrease over time, suggesting progressive decline of left ventricular function [75•].

Myocardial Strain

Clinically significant CTRCD-associated myocardial strain has previously been defined as > 15% deterioration using speckle tracking strain analysis [64]. It however remains unclear how these values translate to CMR measurement. Strain analysis in CMR is well established, with additional features such as myocardial tagging, PVM and feature tracking, which can be easily derived from standard cine SSFP images [96, 97]. Studies using CMR strain analysis to screen patients' CTRCD featured reduced longitudinal deformation and impaired diastolic function with globally reduced LVEF in conjunction with a rise of serological cardiac biomarkers, including troponin and NT-proBNP [85, 98–100].

Similar to LVEF, strain measurements using CMR may detect subclinical myocardial dysfunction. This feature was analysed further in a recent study using strain to detect CTRCD-associated strain deterioration in breast cancer patients receiving trastuzumab with chemotherapy [81]. Results showed a small but significant reduction of LVEF at 6 months but not at 18 months with a parallel decrease of global longitudinal strain (GLS) and global circumferential strain (GCS) at 6 and 12 months after therapy initiation.

Correlations between global strain and LVEF at 6 months were observed (Pearson's $r = -0.60$ and $r = -0.75$ for GLS and GCS, respectively, all $p < 0.001$), highlighting strain measurements in CMR as an additional promising method to monitor prognostic and therapeutic developments in CTRCD.

A further study analysing strain parameters using CMR in patients with CTRCD showed progressive decrease of GLS 3 months and more than 12 months post-treatment (≤ 3 months, 21% ± 8%; ≥ 12 months, 17% ± 11%) compared to healthy controls (24% ± 5%; $p < 0.001$) [75•]. Decreased GLS, which was paralleled by increased native T1 and higher serum NT-proBNP, is indicative of myocardial impairment and remodelling due to diffuse interstitial fibrosis, thus introducing an imaging biosignature to detect CTRCD in early and late stages. Structural and functional LV remodelling was more pronounced in the late (> 12 months) toxicity group. This is because early remodelling is generally more challenging to detect as it is preload-dependent and concealed by depletion of intravascular volume [6•, 64].

Future directions in CMR strain measurements include the development of automated software assessments, which, apart from being highly reproducible, also facilitate image processing in clinical practice. A recent study investigated the efficacy of a new software algorithm featuring rapid 6-min-automated assessments of LV mean mid-wall circumferential strain and LVEF in cine balanced SSFP acquisitions, which was performed on 72 patients with breast cancer, lymphoma and sarcoma [82]. Results revealed a correlation between automated LV strain assessments from cine imaging and conventionally acquired subclinical declines in LVEF ($r = -0.61$; $p < 0.0001$), thus emphasising the effectiveness and ease of using CMR strain measurements in follow-up monitoring of CTRCD. These results offer insight into the potential efficacy and standardisation of myocardial strain measurements by CMR.

Usage of LGE in the Detection of CTRCD

CMR imaging is not routinely used in the detection of CTRCD based on the argumentation that it is not widely available, although it provides several important advantages in CTRCD. The LGE findings are particularly rare in young cancer-patient population, whereas they occur more common in older patients with pre-existing conditions, such as ischaemic heart disease. The chemotoxic cardiomyopathy itself usually manifests in LV dysfunction and remodelling; as such, it promotes build-up of interstitial rather than focal replacement fibrosis, with overall low prevalence of ischaemic-type scarring [17, 101]. A recent study by Kimball et al. investigating 46 breast cancer patients receiving either trastuzumab or a combination with anthracyclines displayed minimal diffuse and no replacement fibrosis as demonstrated by LGE [77]. Another recent investigation comparing early and late cardiotoxic involvement in CTRCD patients similarly showed no statistically significant LGE involvement (5.7% vs. 7.1%; $p > 0.05$) [75•]. Earlier studies came to the same conclusion, with LGE being an infrequent finding amongst anthracycline-associated cardiomyopathy [89–91]. Whereas the studies concluded there were no specific LGE patterns for chemotoxic cardiomyopathy, LGE findings are usually similar to those found in non-ischaemic cardiomyopathy which include midmyocardial, right ventricular insertion point and epicardial locations [70, 102, 103]. Despite these unspecific findings, scar imaging using LGE and ischaemia testing by myocardial perfusion may be particularly useful to screen patients prior to receiving potential cardiotoxic antineoplastic therapy, as it provides valuable clinical information on cardiovascular comorbidities which are associated with poorer outcome of CTRCD [6•]. This highlights the utility of an LGE protocol before the initiation of antineoplastic treatment in order to enable timely initiation of cardiac prevention or intervention.

Quantitative Tissue Characterisation with Myocardial Relaxation Mapping

T1 and T2 mapping are emerging myocardial tissue measures which can be utilised in in-depth characterisation of myocardial pathological processes, such as interstitial fibrosis, infiltration or oedema [104, 105] (Fig. 2). Native T1 is a sensitive parameter to detect abnormal myocardium, reacting to both fibrosis and oedema [106–108]. T2 mapping, on the other hand, is water-specific, thus acting as a direct measure of myocardial oedema and inflammation [109, 110]. The combination of both T1 and T2 mapping therefore holds potential as a diagnostic algorithm for tissue characterisation in CTRCD.

A number of recent studies utilising these novel CMR parameters underscore their potential to detect early- and late-stage CTRCD, as well as monitor its temporal evolution [95•]. Several retrospective investigations showed significantly increased T1 mapping values, indicative of diffusely abnormal myocardial involvement [85, 88, 89, 111]. These findings were previously validated in an experimental study using T1 and T2 mapping as tissue characterisation biomarkers, showing early myocardial inflammation followed by diffuse fibrosis [112]. Increased T1 mapping values were first observed in cancer survivals presenting with suspected late-onset CTRCD by Jordan et al. suggesting they may serve as markers of fibrotic change to monitor the extent of CTRCD in long-term cancer survivors [85].

In addition, T1 in combination with T2 mapping, specific measures of myocardial inflammation, may be instrumental as a diagnostic algorithm to elucidate the temporal evolution of cardiotoxicity [75•]. One hundred fifteen patients with various neoplastic diseases underwent a standardised CMR protocol including measurement of cardiac volumes, mass, T1 and T2 mapping, myocardial perfusion and late gadolinium

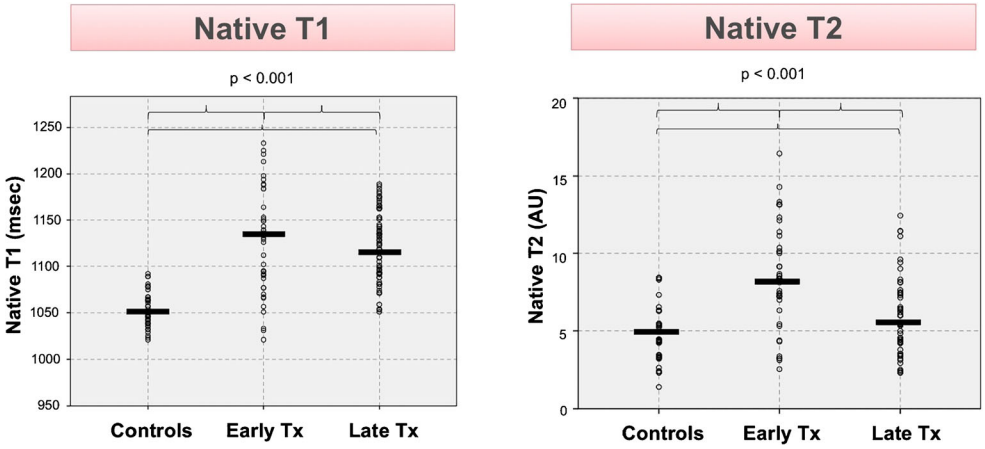

Fig. 4 Median myocardial native T1 and T2 values (msec) in cancer patients receiving treatment within 3 months (early Tx) or 12 months (late Tx). Native T1 values were revealed to be significantly higher than controls in both early and late toxicity groups ($p < 0.001$). Patients receiving treatment within 3 months (early Tx) display higher median T2 values than controls. T2 values then decrease towards baseline value by 12 months (late Tx) ($p < 0.001$), indicating that myocardial oedema develops early treatment and subsides at a later stage. Reprinted from Haslbauer et al. (2018) [75], with permission

enhancement either within 3 months or more than 12 months post-treatment. Results revealed distinct phenotypical biosignatures of early inflammatory involvement (raised native T1 and T2, the hallmark of acute myocardial injury [106, 109]) and interstitial fibrosis and remodelling (raised native T1 but not T2 [107]), thus clearly quantifying the typical sequential clinical manifestations of CTRCD (Fig. 4). For further validation, these findings were analysed in a head-to-head comparison with serum biomarkers; correlations were observed between native T1 and hs-troponin in early disease

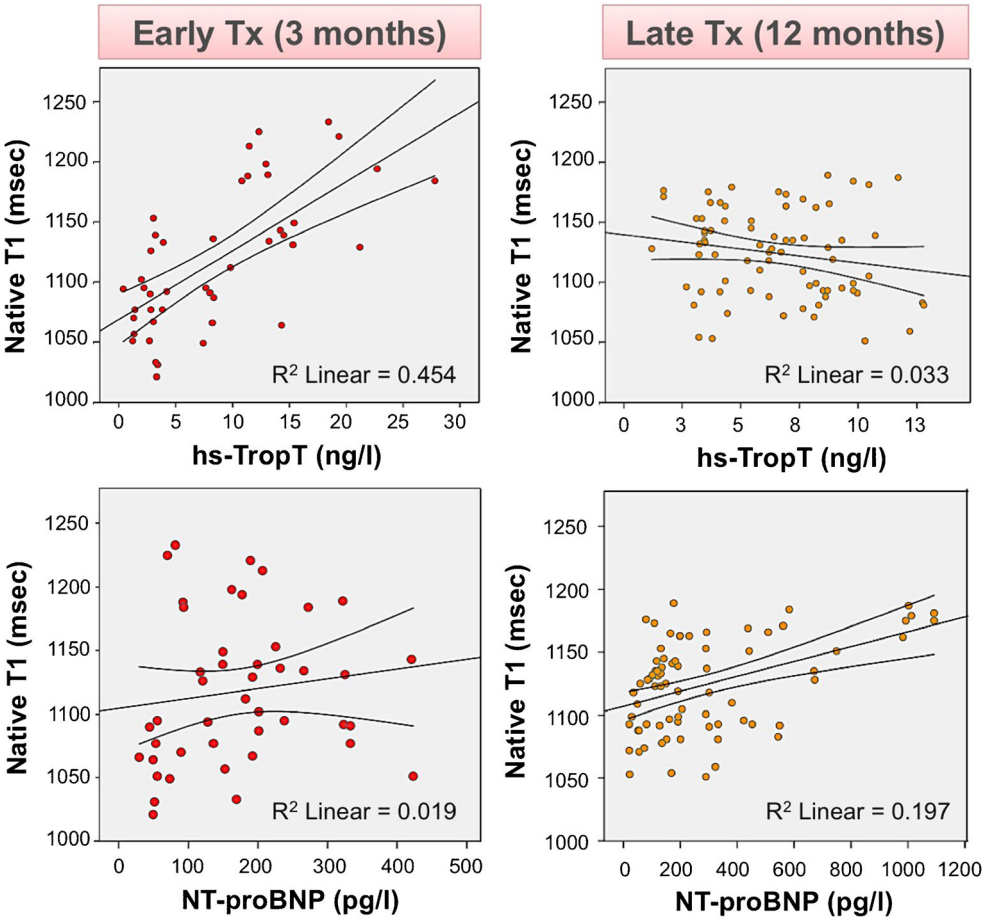

Fig. 5 Correlation of NT-proBNP (pg/L) with T1 mapping in early (3 months) vs. late stages (> 12 months) in post-cancer-related treatment. In cancer patients undergoing CMR within 3 months of receiving treatment, a positive correlation was observed with hs-TropT ($r^2 = 0.454$) but not NT-proBNP, suggesting a profile of acute myocardial injury. This then progresses to diffuse fibrotic remodelling, as evidenced by a positive correlation between T1 values and NT-proBNP in the late toxicity group (12 months post-treatment) ($r^2 = 0.197$) but not hs-TropT. These findings clearly quantify the temporal evolution CTRCD, which typically commences with acute oedematous infiltration, followed by fibrotic disease (see Fig. 1). Reprinted from Haslbauer et al. (2018) [75], with permission

($r^2 = 0.454$) and with NT-proBNP in late disease ($r^2 = 0.197$) (Fig. 5).

Prospective validation in an independent cohort of patients with similar treatment regimens ($n = 25$) and longitudinal assessments further corroborated the biosignatures described above. These patients received CMR screening in conjunction with serological testing of NT-proBNP and hs-TropT at monthly intervals up to 2 years after receiving treatment; results were subsequently compared and contrasted with the original cohort. Within the first month, T2 and hs-TropT were high, suggesting acute myocardial injury and inflammation. Screening conducted at later stages post-therapy revealed steadily decreasing T2 and hs-TropT, which were replaced by an increase of native T1 and NT-proBNP indicative for fibrotic remodelling (Fig. 6). The above data confirms that T1 in conjunction with T2 mapping has potential to accurately and non-invasively quantify

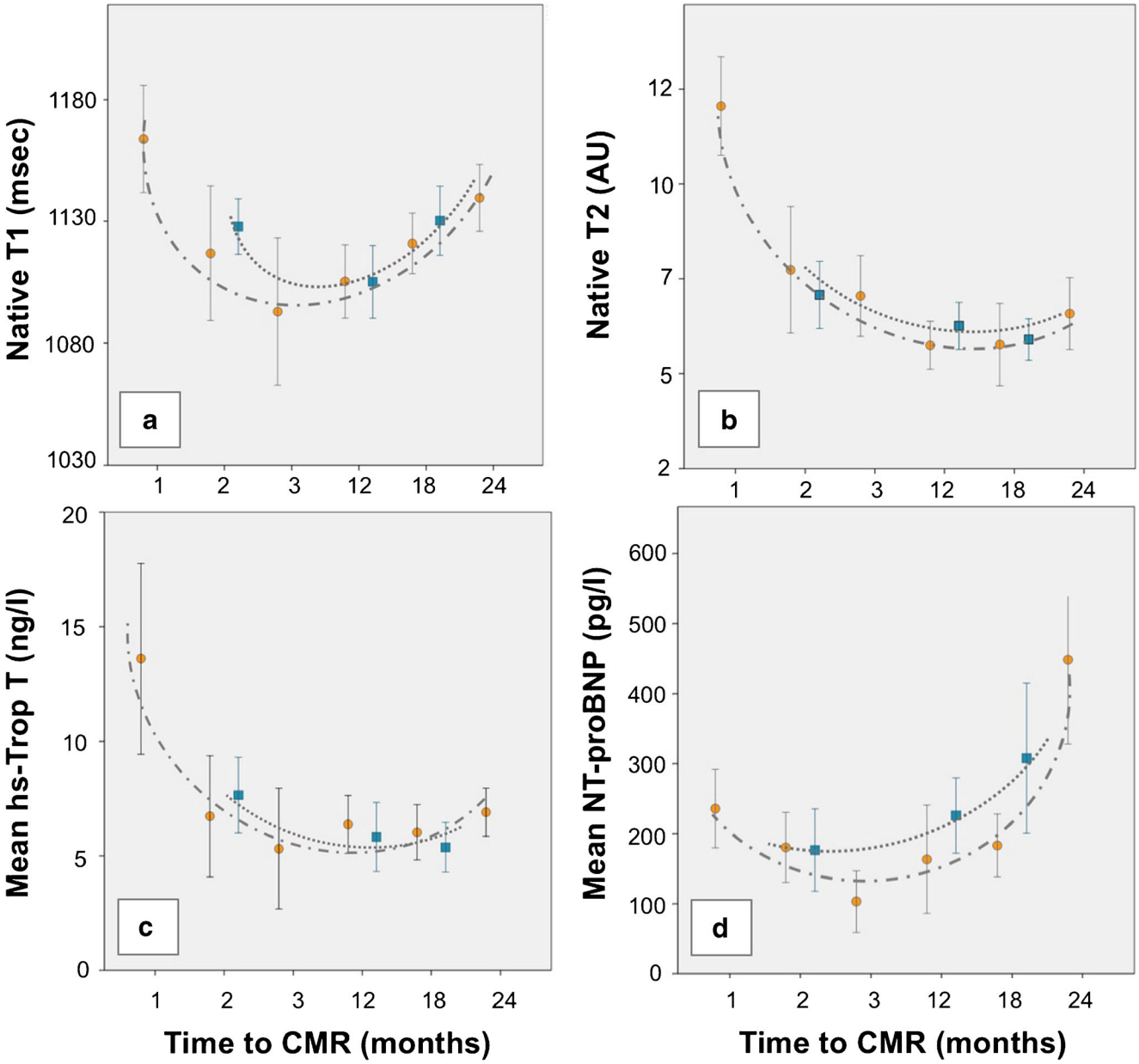

Fig. 6 A comparison of CMR temporal evolution in a longitudinal cohort ($n = 25$) with the original cohort ($n = 115$) in patients receiving antineoplastic therapy. **a**, **d** Mean native T1 and NT-proBNP. **a** Native T1 values were high in early months after receiving antineoplastic therapy, decreasing at approximately 3 months post-therapy in both longitudinal and original cohorts. At 12–24 months after treatment, they begin to again increase, indicating fibrotic change. **d** These developments are mirrored by changes in NT-proBNP. **b**, **c** Mean native T2 and hs-TropT—T2 and troponin both show contrasting findings upon longitudinal comparison. High native T2 and hs-TropT values were measured in early stages post-treatment (1 month), but decreased steadily over time in both cohorts. **b**, **c** Orange = original cohort, blue = longitudinal cohort. Reprinted from Haslbauer et al. (2018) [75], with permission

myocardial inflammation and fibrosis, capturing subclinical changes of CTRCD as well as pharmacologic and patient-specific heterogeneity. Incorporating T1 and T2 mapping into a CMR screening protocol therefore allows non-invasive monitoring of myocardial involvement in both early and late disease. It enables timely administration of cardio-protective treatment measures, thus paving the way towards personalised medicine in CTRCD management.

Other Specific Types of CTRCD

As more advanced antineoplastic agents are developed, there is a growing need to detect, understand and monitor the nature of their potential cardiotoxicity. The underlying heterogeneity of clinical presentation and pathophysiology warrant future in-depth investigation into different treatment modalities; two of which are discussed below.

Immune Checkpoint Inhibitor–Associated Cardiomyopathy

Immune checkpoint inhibitors targeting CTLA-4 (ipilimumab) and the PD-L1/PD-1 pathway (nivolumab, pembrolizumab) have revolutionised the treatment of some types of cancers, such as melanoma, renal cell carcinoma and NSCLC, with many clinical trials currently being conducted to broaden their indications. However, a number of cardiovascular adverse events have been reported in association with these agents, notably as individual case reports of fulminant myocarditis, pericardial disease and vasculitis [63]; their underlying pathogenicity is currently not fully understood. Though their incidence is rare comparing to other adverse events, fatality rates of cardiovascular complications are high: according to an observational study by Moslehi et al., myocarditis resulting from combination therapy of anti-PD-1/PD-L1 and CTLA-4 inhibition revealed higher mortality than anti-PD-1/PD-L1 monotherapy (78% vs. 42%; $p = 0.004$) [113]. Lack of treatment efficacy, as well as heterogeneity in clinical presentation, presents an urgent need for early detection and management.

CMR may be an effective diagnostic tool, given its utility as a gold standard in myocarditis management; however, there currently are no clinical investigations involving CMR in the field of immune checkpoint–mediated cardiotoxicity, although some case studies have tapped on its potential. A case report by Löffler and Salerno [65] features a melanoma patient receiving a combination therapy of ipilimumab/nivolumab who developed tachycardia, palpitations and pre-syncope after treatment. CMR revealed elevated T1 and T2 and subepicardial LGE, consistent with acute myocarditis.

Future interdisciplinary research, both basic and clinical in approach, is needed to elucidate the mechanisms of immune-myocardial crosstalk and to identify CV, autoimmune, tumour and genetic factors associated with a higher risk to develop CTRCD. These efforts, in conjunction with highly sensitive diagnostic tools like CMR, will help to develop an algorithm to effectively manage cardiovascular events associated with these agents.

Radiation-Associated Cardiomyopathy

Cardiac dysfunction linked to radiation is typically a late complication and mostly manifests as acute/constrictive

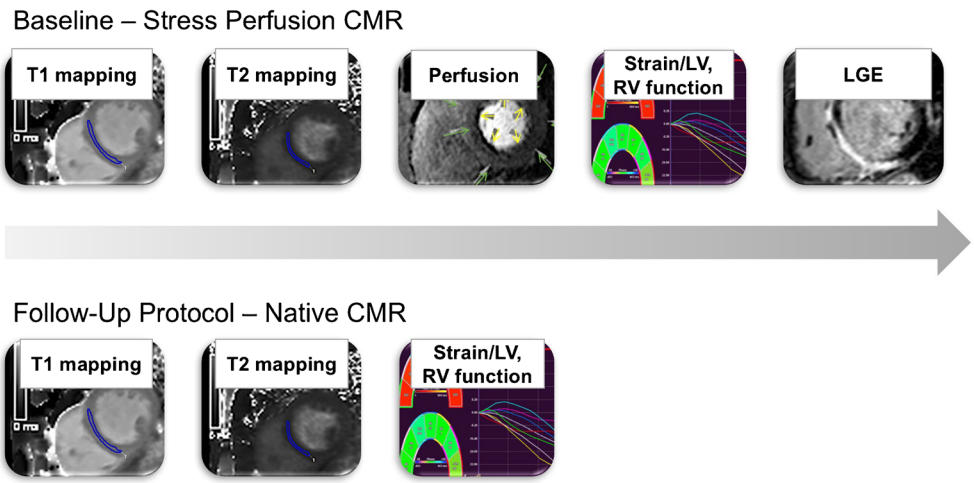

Fig. 7 CMR baseline and follow-up protocols for patients with CTRCD. This diagram illustrates suggested CMR imaging protocols for patients undergoing antineoplastic treatment regimes. We recommend baseline CMR examination with T1 and T2 parametric mapping followed by myocardial perfusion, strain (LV/RV function) and LGE prior to therapy initiation for comprehensive assessment of cardiac function as well as screening for cardiovascular comorbidities. Several follow-up protocols within the first 3 months of receiving therapy allows timely detection of myocardial injury and/or inflammation, as well as subclinical disease. LV = left ventricular, LGE = late gadolinium enhancement. Adapted from Haslbauer et al. (2018) [75], with permission

pericarditis. A further complication characteristically associated with mediastinal radiation in particular is restrictive cardiomyopathy [5, 65].

Clinical studies investigating the extent and monitoring of radiation-associated cardiomyopathy amount to a case study of a patient with oesophageal cancer who developed left ventricular systolic and diastolic dysfunction as a result of radiation therapy [114]. T1 mapping depicted global myocardial fibrosis which was confirmed by subsequent EMB analysis revealing interstitial fibrosis. This case shows the potential of native and post-contrast T1 mapping by CMR to effectively assess radiation-induced cardiomyopathy by enabling the estimation extracellular volume (ECV), which is elevated in diffuse myocardial fibrosis. T1 mapping therefore was shown to be useful for early detection of radiation-associated myocardial damage, although future clinical trials are required to measure its utility in daily clinical practice.

Future Directions and Conclusion

With the development of novel antineoplastic therapies, cardio-oncology has become a cornerstone in cardiovascular research to preserve survival and quality of life in the era of personalised medicine. The prospects of CMR as a tool for cardiovascular surveillance are promising, especially due to its unique ability to identify biosignatures and distinct morphological patterns of myocardial damage. Furthermore, its objective and reproducible measurement of ventricular function and changes in myocardial strain highlight its potentially valuable role in the detection of CTRCD for early detection and prophylaxis [99, 100]. We therefore propose the introduction of a standard CMR protocol for initial screening before treatment initiation and for follow-up after receiving cardiotoxic therapy, including assessment of baseline native T1 and T2 values, GLS and LGE (Fig. 7). Moreover, this would be an effective method to limit exposure to kidney-damaging contrast agents in a patient population prone to receiving a substantial amount of radiation-based diagnostics [115]. Consequently, CMR can be used as a supportive diagnostic tool in several recent cardio-oncological studies. T1 mapping, in conjunction with serum biomarkers and next-generation sequencing, has been used in a promising multi-centre observational study to identify genomic risk factors associated with CTRCD [116]. A further study investigating the efficacy of metoprolol and candesartan treating anthracycline cardiotoxicity in breast cancer patients used CMR as a monitoring tool to detect changes in T1 mapping before and after administration of cardio-protective treatment [117]. Results revealed that concomitant treatment with candesartan reduced left ventricular total cellular volume, suggesting reduction of intracellular oedema. These examples illustrate the utility for a flexible and sensitive image modality like CMR in this constantly evolving field of study.

In conclusion, the need for multi-modality cardiovascular imaging like CMR forms an integral part in future investigations in cardio-oncology, paving the way towards effective identification of susceptible myocardium, understanding of toxicity phenotypes and allowing appropriate initiation of cardio-protective treatment.

Compliance with Ethical Standards

Conflict of Interest Jasmin D. Haslbauer, Gesine Bug, Eike Nagel and Valentina O. Puntmann declare that they have no conflict of interest.

Sarah Lindner receives travel support from Celgene, Sanofi and Neovii.

Human and Animal Rights and Informed Consent This article does not contain any studies with human or animal subjects performed by any of the authors.

References

Papers of particular interest, published recently, have been highlighted as:

- Of importance

1. Hashim D, Boffetta P, La Vecchia C, Rota M, Bertuccio P, Malvezzi M, et al. The global decrease in cancer mortality: trends and disparities. Ann Oncol. 2016;27(5):926–33.
2. Siegel RL, Miller KD, Jemal A. Cancer statistics, 2018. CA Cancer J Clin. 2018;68(1):7–30.
3. Manrique CR, Park M, Tiwari N, Plana JC, Garcia MJ. Diagnostic strategies for early recognition of cancer therapeutics-related cardiac dysfunction. Clin Med Insights Cardiol. 2017;11:1179546817697983.
4. Koutsoukis A, Ntalianis A, Repasos E, Kastritis E, Dimopoulos M-A, Paraskevaidis I. Cardio-oncology: a focus on cardiotoxicity. Eur Cardiol. 2018;13(1):64–9.
5. Plana JC, Thavendiranathan P, Bucciarelli-Ducci C, Lancellotti P. Multi-modality imaging in the assessment of cardiovascular toxicity in the cancer patient. JACC Cardiovasc Imaging. 2018;11(8):1173–86.
6. • Zamorano JL, Lancellotti P, Rodriguez Muñoz D, Aboyans V, Asteggiano R, Galderisi M, et al. 2016 ESC Position Paper on cancer treatments and cardiovascular toxicity developed under the auspices of the ESC Committee for Practice Guidelines: the task force for cancer treatments and cardiovascular toxicity of the European Society of Cardiology (ESC). Eur Heart J. 2016;37(36):2768–801 **This ESC practice guideline provides an in-depth, critical review on current diagnostic tools to screen, diagnose and manage patients with CTRCD**.
7. Kostakou PM, Kouris NT, Kostopoulos VS, Damaskos DS, Olympios CD. Cardio-oncology: a new and developing sector of research and therapy in the field of cardiology. Heart Fail Rev 2018

8. McGowan JV, Chung R, Maulik A, Piotrowska I, Walker JM, Yellon DM. Anthracycline chemotherapy and cardiotoxicity. Cardiovasc Drugs Ther. 2017;31(1):63–75.
9. Pai VB, Nahata MC. Cardiotoxicity of chemotherapeutic agents: incidence, treatment and prevention. Drug Saf. 2000;22(4):263–302.
10. Jain D, Ahmad T, Cairo M, Aronow W. Cardiotoxicity of cancer chemotherapy: identification, prevention and treatment. Ann Transl Med [Internet]. 2017[cited 2018 May 25];5(17). Available from: https://www.ncbi.nlm.nih.gov/pmc/articles/PMC5599271/
11. Zeglinski M, Ludke A, Jassal DS, Singal PK. Trastuzumab-induced cardiac dysfunction: a 'dual-hit'. Exp Clin Cardiol. 2011;16(3):70–4.
12. Lee W-S, Kim J. Cardiotoxicity associated with tyrosine kinase-targeted anticancer therapy. Mol Cell Toxicol. 2018;14(3):247–54.
13. Gilda V, Rosaria GM, Tocchetti Carlo G. Cardiac toxicity of immune checkpoint inhibitors. Circulation. 2017;136(21):1989–92.
14. Hamo CE, Bloom MW. Getting to the heart of the matter: an overview of cardiac toxicity related to cancer therapy. Clin Med Insights Cardiol. 2015;9(Suppl 2):47–51.
15. Sawyer DB, Peng X, Chen B, Pentassuglia L, Lim CC. Mechanisms of anthracycline cardiac injury: can we identify strategies for cardio-protection? Prog Cardiovasc Dis. 2010;53(2):105–13.
16. Berry GJ, Jorden M. Pathology of radiation and anthracycline cardiotoxicity. Pediatr Blood Cancer. 2005;44(7):630–7.
17. Bernaba BN, Chan JB, Lai CK, Fishbein MC. Pathology of late-onset anthracycline cardiomyopathy. Cardiovasc Pathol Off J Soc Cardiovasc Pathol. 2010;19(5):308–11.
18. Lemmens K, Doggen K, De Keulenaer GW. Role of neuregulin-1/ErbB signaling in cardiovascular physiology and disease: implications for therapy of heart failure. Circulation. 2007;116(8):954–60.
19. Florido R, Smith KL, Cuomo KK, Russell SD. Cardiotoxicity from human epidermal growth factor receptor-2 (HER2) targeted therapies. J Am Heart Assoc Cardiovasc Cerebrovasc Dis [Internet]. 2017[cited 2018 Nov 25];6(9). Available from: https://www.ncbi.nlm.nih.gov/pmc/articles/PMC5634312/
20. Chen J, Long JB, Hurria A, Owusu C, Steingart RM, Gross CP. Incidence of heart failure or cardiomyopathy after adjuvant trastuzumab therapy for breast cancer. J Am Coll Cardiol. 2012;60(24):2504–12.
21. Bloom MW, Hamo CE, Cardinale D, Ky B, Nohria A, Baer L, et al. Cancer therapy-related cardiac dysfunction and heart failure part 1: definitions, pathophysiology, risk factors, and imaging. Circ Heart Fail. 2016;9(1):e002661.
22. Tanaka S, Ikari A, Nitta T, Horiuchi T. Long-term irreversible trastuzumab-induced cardiotoxicity for metastatic breast cancer in a patient without cardiac risk factors. Oxf Med Case Rep [Internet]. 2017[cited 2018 Nov 25];2017(7). Available from: https://www.ncbi.nlm.nih.gov/pmc/articles/PMC5499211/
23. Slamon D, Eiermann W, Robert N, Pienkowski T, Martin M, Press M, et al. Adjuvant trastuzumab in HER2-positive breast cancer. N Engl J Med. 2011;365(14):1273–83.
24. Romond EH, Perez EA, Bryant J, Suman VJ, Geyer CE, Davidson NE, et al. Trastuzumab plus adjuvant chemotherapy for operable HER2-positive breast cancer. N Engl J Med. 2005;353(16):1673–84.
25. Martin M, Pienkowski T, Mackey J, Pawlicki M, Guastalla J-P, Weaver C, et al. Adjuvant docetaxel for node-positive breast cancer. N Engl J Med. 2005;352(22):2302–13.
26. Martín M, Seguí MA, Antón A, Ruiz A, Ramos M, Adrover E, et al. Adjuvant docetaxel for high-risk, node-negative breast cancer. N Engl J Med. 2010;363(23):2200–10.
27. Fisher B, Jeong J-H, Dignam J, Anderson S, Mamounas E, Wickerham DL, et al. Findings from recent National Surgical Adjuvant Breast and Bowel Project adjuvant studies in stage I breast cancer. JNCI Monogr. 2001;2001(30):62–6.
28. Martin M, Villar A, Sole-Calvo A, Gonzalez R, Massuti B, Lizon J, et al. Doxorubicin in combination with fluorouracil and cyclophosphamide (i.v. FAC regimen, day 1, 21) versus methotrexate in combination with fluorouracil and cyclophosphamide (i.v. CMF regimen, day 1, 21) as adjuvant chemotherapy for operable breast cancer: a study by the GEICAM group. Ann Oncol Off J Eur Soc Med Oncol. 2003;14(6):833–42.
29. Sparano JA, Wang M, Martino S, Jones V, Perez EA, Saphner T, et al. Weekly paclitaxel in the adjuvant treatment of breast cancer. N Engl J Med. 2008;358(16):1663–71.
30. Roché H, Fumoleau P, Spielmann M, Canon J-L, Delozier T, Serin D, et al. Sequential adjuvant epirubicin-based and docetaxel chemotherapy for node-positive breast cancer patients: the FNCLCC PACS 01 trial. J Clin Oncol Off J Am Soc Clin Oncol. 2006;24(36):5664–71.
31. Citron ML, Berry DA, Cirrincione C, Hudis C, Winer EP, Gradishar WJ, et al. Randomized trial of dose-dense versus conventionally scheduled and sequential versus concurrent combination chemotherapy as postoperative adjuvant treatment of node-positive primary breast cancer: first report of Intergroup Trial C9741/Cancer and Leukemia Group B Trial 9741. J Clin Oncol Off J Am Soc Clin Oncol. 2003;21(8):1431–9.
32. Sessa C, Pagani O. Docetaxel and epirubicin in advanced breast cancer. Oncologist. 2001;6(Supplement 3):13–6.
33. Julka PK, Awasthy BS, Sharma DN, Gairola M, Rath GK. Paclitaxel-epirubicin in advanced breast cancer. J Assoc Physicians India. 1999;47(5):499–502.
34. Gehl J, Boesgaard M, Paaske T, Vittrup Jensen B, Dombernowsky P. Combined doxorubicin and paclitaxel in advanced breast cancer: effective and cardiotoxic. Ann Oncol Off J Eur Soc Med Oncol. 1996;7(7):687–93.
35. Baltali E, Ozişik Y, Güler N, Firat D, Altundağ K. Combination of docetaxel and doxorubicin as first-line chemotherapy in metastatic breast cancer. Tumori. 2001;87(1):18–9.
36. Chan S, Davidson N, Juozaityte E, Erdkamp F, Pluzanska A, Azarnia N, et al. Phase III trial of liposomal doxorubicin and cyclophosphamide compared with epirubicin and cyclophosphamide as first-line therapy for metastatic breast cancer. Ann Oncol Off J Eur Soc Med Oncol. 2004;15(10):1527–34.
37. Monk BJ, Herzog TJ, Kaye SB, Krasner CN, Vermorken JB, Muggia FM, et al. Trabectedin plus pegylated liposomal doxorubicin in recurrent ovarian cancer. J Clin Oncol Off J Am Soc Clin Oncol. 2010;28(19):3107–14.
38. Ueda Y, Miyake T, Egawa-Takata T, Miyatake T, Matsuzaki S, Yokoyama T, et al. Second-line chemotherapy for advanced or recurrent endometrial carcinoma previously treated with paclitaxel and carboplatin, with or without epirubicin. Cancer Chemother Pharmacol. 2011;67(4):829–35.
39. He Q, Zhao J, Yuan J, Gong Z, Yi T. Combined perioperative EOX chemotherapy and postoperative chemoradiotherapy for locally advanced gastric cancer. Mol Clin Oncol. 2017;7(2):211–6.
40. Gunturu KS, Woo Y, Beaubier N, Remotti HE, Saif MW. Gastric cancer and trastuzumab: first biologic therapy in gastric cancer. Ther Adv Med Oncol. 2013;5(2):143–51.
41. Chan BA, Coward JIG. Chemotherapy advances in small-cell lung cancer. J Thorac Dis. 2013;5(Suppl 5):S565–78.
42. Pacini F, Castagna MG, Brilli L, Pentheroudakis G, ESMO Guidelines Working Group. Thyroid cancer: ESMO Clinical Practice Guidelines for diagnosis, treatment and follow-up. Ann Oncol Off J Eur Soc Med Oncol. 2010;21(Suppl 5):v214–9.
43. Okuno SH, Mailliard JA, Suman VJ, Edmonson JH, Creagan ET, Nair S, et al. Phase II study of methotrexate, vinblastine, doxorubicin, and cisplatin in patients with squamous cell carcinoma of

the upper respiratory or alimentary passages of the head and neck. Cancer. 2002;94(8):2224–31.
44. Hoelzer D, Bassan R, Dombret H, Fielding A, Ribera JM, Buske C, et al. Acute lymphoblastic leukaemia in adult patients: ESMO Clinical Practice Guidelines for diagnosis, treatment and follow-up. Ann Oncol Off J Eur Soc Med Oncol. 2016;27(suppl 5):v69–82.
45. Fey MF, Buske C, ESMO Guidelines Working Group. Acute myeloblastic leukaemias in adult patients: ESMO Clinical Practice Guidelines for diagnosis, treatment and follow-up. Ann Oncol Off J Eur Soc Med Oncol. 2013;24(Suppl 6):vi138–43.
46. Oakervee HE, Popat R, Curry N, Smith P, Morris C, Drake M, et al. PAD combination therapy (PS-341/bortezomib, doxorubicin and dexamethasone) for previously untreated patients with multiple myeloma. Br J Haematol. 2005;129(6):755–62.
47. Boleti E, Mead GM. ABVD for Hodgkin's lymphoma: full-dose chemotherapy without dose reductions or growth factors. Ann Oncol. 2007;18(2):376–80.
48. Kelly KM, Sposto R, Hutchinson R, Massey V, McCarten K, Perkins S, et al. BEACOPP chemotherapy is a highly effective regimen in children and adolescents with high-risk Hodgkin lymphoma: a report from the Children's Oncology Group. Blood. 2011;117(9):2596–603.
49. Fisher RI, Gaynor ER, Dahlberg S, Oken MM, Grogan TM, Mize EM, et al. Comparison of a standard regimen (CHOP) with three intensive chemotherapy regimens for advanced non-Hodgkin's lymphoma. N Engl J Med. 1993;328(14):1002–6.
50. Pfreundschuh M, Zwick C, Zeynalova S, Duhrsen U, Pfluger K-H, Vrieling T, et al. Dose-escalated CHOEP for the treatment of young patients with aggressive non-Hodgkin's lymphoma: II. Results of the randomized high-CHOEP trial of the German High-Grade Non-Hodgkin's Lymphoma Study Group (DSHNHL). Ann Oncol. 2007;19(3):545–52.
51. Keating GM. Pixantrone: a review in relapsed or refractory aggressive non-Hodgkin's lymphoma. Drugs. 2016;76(16):1579–86.
52. Information NC for B, Pike USNL of M 8600 R, MD B, Usa 20894. Evidence and recommendations on Kaposi sarcoma (KS) [Internet]. World Health Organization; 2014 [cited 2018 Dec 10]. Available from: http://www.ncbi.nlm.nih.gov/books/NBK305418/
53. Sagaster P, Flamm J, Flamm M, Mayer A, Donner G, Oberleitner S, et al. Neoadjuvant chemotherapy (MVAC) in locally invasive bladder cancer. Eur J Cancer Oxf Engl 1990. 1996;32A(8):1320–4.
54. Bamias A, Dimitriadis I. Systemic chemotherapy for urothelial cancer – how to select systemic therapy in bladder cancer. Syst Chemother Urothelial Cancer – Sel Syst Ther Bladder Cancer [Internet]. 2017 [cited 2018 Dec 10]; Available from: https://www.touchoncology.com/articles/systemic-chemotherapy-urothelial-cancer-how-select-systemic-therapy-bladder-cancer
55. Dangoor A, Seddon B, Gerrand C, Grimer R, Whelan J, Judson I. UK guidelines for the management of soft tissue sarcomas. Clin Sarcoma Res. 2016;6(1):20.
56. Pender A, Jones RL. Olaratumab: a platelet-derived growth factor receptor-α-blocking antibody for the treatment of soft tissue sarcoma. Clin Pharmacol Adv Appl. 2017;9:159–64.
57. Whelan J, Khan A, Sharma A, Rothermundt C, Dileo P, Michelagnoli M, et al. Interval compressed vincristine, doxorubicin, cyclophosphamide alternating with ifosfamide, etoposide in patients with advanced Ewing's and other small round cell sarcomas. Clin Sarcoma Res. 2012;2:12.
58. Kleinerman E. Maximum benefit of chemotherapy for osteosarcoma achieved—what are the next steps? Lancet Oncol. 2016;17(10):1340–2.
59. Bhatnagar S. Management of Wilms' tumor: NWTS vs SIOP. J Indian Assoc Pediatr Surg. 2009;14(1):6–14.
60. McWilliams NB, Hayes FA, Green AA, Smith EI, Nitschke R, Altshuler GA, et al. Cyclophosphamide/doxorubicin vs. cisplatin/teniposide in the treatment of children older than 12 months of age with disseminated neuroblastoma: a pediatric oncology group randomized phase II study. Med Pediatr Oncol. 1995;24(3):176–80.
61. Amoroso L, Erminio G, Makin G, Pearson ADJ, Brock P, Valteau-Couanet D, et al. Topotecan-vincristine-doxorubicin in stage 4 high-risk neuroblastoma patients failing to achieve a complete metastatic response to rapid COJEC: a SIOPEN study. Cancer Res Treat. 2017;50(1):148–55.
62. Orphanos GS, Ioannidis GN, Ardavanis AG. Cardiotoxicity induced by tyrosine kinase inhibitors. Acta Oncol Stockh Swed. 2009;48(7):964–70.
63. Varricchi G, Galdiero MR, Marone G, Criscuolo G, Triassi M, Bonaduce D, et al. Cardiotoxicity of immune checkpoint inhibitors. ESMO Open [Internet]. 2017[cited 2018 Nov 18];2(4). Available from: https://www.ncbi.nlm.nih.gov/pmc/articles/PMC5663252/
64. Plana JC, Galderisi M, Barac A, Ewer MS, Ky B, Scherrer-Crosbie M, et al. Expert consensus for multimodality imaging evaluation of adult patients during and after cancer therapy: a report from the American Society of Echocardiography and the European Association of Cardiovascular Imaging. J Am Soc Echocardiogr Off Publ Am Soc Echocardiogr. 2014;27(9):911–39.
65. Löffler AI, Salerno M. Cardiac MRI for the evaluation of oncologic cardiotoxicity. J Nucl Cardiol Off Publ Am Soc Nucl Cardiol 2018.
66. Thavendiranathan P, Wintersperger BJ, Flamm SD, Marwick TH. Cardiac MRI in the assessment of cardiac injury and toxicity from cancer chemotherapy: a systematic review. Circ Cardiovasc Imaging. 2013;6(6):1080–91.
67. Oreto L, Todaro MC, Umland MM, Kramer C, Qamar R, Carerj S, et al. Use of echocardiography to evaluate the cardiac effects of therapies used in cancer treatment: what do we know? J Am Soc Echocardiogr Off Publ Am Soc Echocardiogr. 2012;25(11):1141–52.
68. Armstrong GT, Plana JC, Zhang N, Srivastava D, Green DM, Ness KK, et al. Screening adult survivors of childhood cancer for cardiomyopathy: comparison of echocardiography and cardiac magnetic resonance imaging. J Clin Oncol Off J Am Soc Clin Oncol. 2012;30(23):2876–84.
69. Armstrong AC, Gidding S, Gjesdal O, Wu C, Bluemke DA, Lima JAC. LV mass assessed by echocardiography and CMR, cardiovascular outcomes, and medical practice. JACC Cardiovasc Imaging. 2012;5(8):837–48.
70. Fallah-Rad N, Walker JR, Wassef A, Lytwyn M, Bohonis S, Fang T, et al. The utility of cardiac biomarkers, tissue velocity and strain imaging, and cardiac magnetic resonance imaging in predicting early left ventricular dysfunction in patients with human epidermal growth factor receptor II-positive breast cancer treated with adjuvant trastuzumab therapy. J Am Coll Cardiol. 2011;57(22):2263–70.
71. Henri C, Heinonen T, Tardif J-C. The role of biomarkers in decreasing risk of cardiac toxicity after cancer therapy. Biomark Cancer. 2016;8(Suppl 2):39–45.
72. Riddell E, Lenihan D. The role of cardiac biomarkers in cardio-oncology. Curr Probl Cancer. 2018;42(4):375–85.
73. Tan L-L, Lyon AR. Role of biomarkers in prediction of cardiotoxicity during cancer treatment. Curr Treat Options Cardiovasc Med [Internet]. 2018 [cited 2018 Nov 25];20(7). Available from: https://www.ncbi.nlm.nih.gov/pmc/articles/PMC6008350/

74. Berridge BR, Pettit S, Walker DB, Jaffe AS, Schultze AE, Herman E, et al. A translational approach to detecting drug-induced cardiac injury with cardiac troponins: consensus and recommendations from the cardiac troponins biomarker working group of the health and environmental sciences institute. Am Heart J. 2009;158(1): 21–9.
75.• Haslbauer JD, Lindner S, Valbuena-Lopez S, Zainal H, Zhou H, D'Angelo T, et al. CMR imaging biosignature of cardiac involvement due to cancer-related treatment by T1 and T2 mapping. Int J Cardiol. 2018. **This study unravels novel imaging biosignatures (T1 and T2 mapping) as a diagnostic algorithm to characterise the extent of myocardial oedema and/or fibrosis in CTRCD patients, thus highlighting the potential of CMR to manage CTRCD.**
76. Gong IY, Ong G, Brezden-Masley C, Dhir V, Deva DP, Chan KKW, et al. Early diastolic strain rate measurements by cardiac MRI in breast cancer patients treated with trastuzumab: a longitudinal study. Int J Card Imaging 2018.
77. Kimball A, Patil S, Koczwara B, Raman KS, Perry R, Grover S, et al. Late characterisation of cardiac effects following anthracycline and trastuzumab treatment in breast cancer patients. Int J Cardiol. 2018;261:159–61.
78. Grover S, Leong DP, Chakrabarty A, Joerg L, Kotasek D, Cheong K, et al. Left and right ventricular effects of anthracycline and trastuzumab chemotherapy: a prospective study using novel cardiac imaging and biochemical markers. Int J Cardiol. 2013;168(6): 5465–7.
79. Ferreira de Souza T, Quinaglia AC, Silva T, Osorio Costa F, Shah R, Neilan TG, et al. Anthracycline therapy is associated with cardiomyocyte atrophy and preclinical manifestations of heart disease. JACC Cardiovasc Imaging. 2018;11(8):1045–55.
80. Muehlberg F, Funk S, Zange L, von Knobelsdorff-Brenkenhoff F, Blaszczyk E, Schulz A, et al. Native myocardial T1 time can predict development of subsequent anthracycline-induced cardiomyopathy. ESC Heart Fail 2018.
81. Ong G, Brezden-Masley C, Dhir V, Deva DP, Chan KKW, Chow C-M, et al. Myocardial strain imaging by cardiac magnetic resonance for detection of subclinical myocardial dysfunction in breast cancer patients receiving trastuzumab and chemotherapy. Int J Cardiol. 2018;261:228–33.
82. Jolly M-P, Jordan JH, Meléndez GC, McNeal GR, D'Agostino RB, Hundley WG. Automated assessments of circumferential strain from cine CMR correlate with LVEF declines in cancer patients early after receipt of cardio-toxic chemotherapy. J Cardiovasc Magn Reson [Internet]. 2017 [cited 2018 Nov 17];19. Available from: https://www.ncbi.nlm.nih.gov/pmc/articles/PMC5541737/
83. Barthur A, Brezden-Masley C, Connelly KA, Dhir V, Chan KKW, Haq R, et al. Longitudinal assessment of right ventricular structure and function by cardiovascular magnetic resonance in breast cancer patients treated with trastuzumab: a prospective observational study. J Cardiovasc Magn Reson Off J Soc Cardiovasc Magn Reson. 2017;19(1):44.
84. Nakano S, Takahashi M, Kimura F, Senoo T, Saeki T, Ueda S, et al. Cardiac magnetic resonance imaging-based myocardial strain study for evaluation of cardiotoxicity in breast cancer patients treated with trastuzumab: a pilot study to evaluate the feasibility of the method. Cardiol J. 2016;23(3):270–80.
85. Jordan JH, Vasu S, Morgan TM, D'Agostino RB, Meléndez GC, Hamilton CA, et al. Anthracycline-associated T1 mapping characteristics are elevated independent of the presence of cardiovascular comorbidities in cancer survivors. Circ Cardiovasc Imaging. 2016;9(8).
86. Grover S, Lou PW, Bradbrook C, Cheong K, Kotasek D, Leong DP, et al. Early and late changes in markers of aortic stiffness with breast cancer therapy. Intern Med J. 2015;45(2):140–7.
87. Drafts BC, Twomley KM, D'Agostino R, Lawrence J, Avis N, Ellis LR, et al. Low to moderate dose anthracycline-based chemotherapy is associated with early noninvasive imaging evidence of subclinical cardiovascular disease. JACC Cardiovasc Imaging. 2013;6(8):877–85.
88. Tham EB, Haykowsky MJ, Chow K, Spavor M, Kaneko S, Khoo NS, et al. Diffuse myocardial fibrosis by T1-mapping in children with subclinical anthracycline cardiotoxicity: relationship to exercise capacity, cumulative dose and remodeling. J Cardiovasc Magn Reson Off J Soc Cardiovasc Magn Reson. 2013;15:48.
89. Neilan TG, Coelho-Filho OR, Pena-Herrera D, Shah RV, Jerosch-Herold M, Francis SA, et al. Left ventricular mass in patients with a cardiomyopathy after treatment with anthracyclines. Am J Cardiol. 2012;110(11):1679–86.
90. Ylänen K, Poutanen T, Savikurki-Heikkilä P, Rinta-Kiikka I, Eerola A, Vettenranta K. Cardiac magnetic resonance imaging in the evaluation of the late effects of anthracyclines among long-term survivors of childhood cancer. J Am Coll Cardiol. 2013;61(14):1539–47.
91. Toro-Salazar OH, Gillan E, O'Loughlin MT, Burke GS, Ferranti J, Stainsby J, et al. Occult cardiotoxicity in childhood cancer survivors exposed to anthracycline therapy. Circ Cardiovasc Imaging. 2013;6(6):873–80.
92. Seidman A, Hudis C, Pierri MK, Shak S, Paton V, Ashby M, et al. Cardiac dysfunction in the trastuzumab clinical trials experience. J Clin Oncol Off J Am Soc Clin Oncol. 2002;20(5):1215–21.
93. Grothues F, Smith GC, Moon JCC, Bellenger NG, Collins P, Klein HU, et al. Comparison of interstudy reproducibility of cardiovascular magnetic resonance with two-dimensional echocardiography in normal subjects and in patients with heart failure or left ventricular hypertrophy. Am J Cardiol. 2002;90(1):29–34.
94. Rasool HJ, Tak T, Gill P, Novotny JE, Jaekel C, Elkhatib RT, et al. Cardiovascular magnetic resonance imaging compared to echocardiogram for detecting doxorubicin-induced cardiotoxicity. J Clin Oncol. 2014;32(15_suppl):1068.
95.• Puntmann VO, Valbuena S, Hinojar R, Petersen SE, Greenwood JP, Kramer CM, et al. Society for Cardiovascular Magnetic Resonance (SCMR) expert consensus for CMR imaging endpoints in clinical research: part I - analytical validation and clinical qualification. J Cardiovasc Magn Reson. 2018;20(1):67 **This SCMR expert consensus offers appraisal on current evidence surrounding CMR imaging endpoints, discussing the key strengths this image modality has to offer, as well as transferability of acquisition and post-processing into clinical practice**.
96. Almutairi HM, Boubertakh R, Miquel ME, Petersen SE. Myocardial deformation assessment using cardiovascular magnetic resonance-feature tracking technique. Br J Radiol. 2017;90(1080):20170072.
97. Scatteia A, Baritussio A, Bucciarelli-Ducci C. Strain imaging using cardiac magnetic resonance. Heart Fail Rev. 2017;22(4): 465–76.
98. Burridge PW, Li YF, Matsa E, Wu H, Ong S-G, Sharma A, et al. Human induced pluripotent stem cell-derived cardiomyocytes recapitulate the predilection of breast cancer patients to doxorubicin-induced cardiotoxicity. Nat Med. 2016;22(5):547–56.
99. Gulati G, Heck SL, Ree AH, Hoffmann P, Schulz-Menger J, Fagerland MW, et al. Prevention of cardiac dysfunction during adjuvant breast cancer therapy (PRADA): a 2 × 2 factorial, randomized, placebo-controlled, double-blind clinical trial of candesartan and metoprolol. Eur Heart J. 2016;37(21):1671–80.
100. Cardinale D, Colombo A, Bacchiani G, Tedeschi I, Meroni CA, Veglia F, et al. Early detection of anthracycline cardiotoxicity and improvement with heart failure therapy. Circulation. 2015;131(22):1981–8.
101. Schulz-Menger J, Bluemke DA, Bremerich J, Flamm SD, Fogel MA, Friedrich MG, et al. Standardized image interpretation and

post processing in cardiovascular magnetic resonance: Society for Cardiovascular Magnetic Resonance (SCMR) board of trustees task force on standardized post processing. J Cardiovasc Magn Reson Off J Soc Cardiovasc Magn Reson. 2013;15:35.

102. Wadhwa D, Fallah-Rad N, Grenier D, Krahn M, Fang T, Ahmadie R, et al. Trastuzumab mediated cardiotoxicity in the setting of adjuvant chemotherapy for breast cancer: a retrospective study. Breast Cancer Res Treat. 2009;117(2):357–64.
103. Fallah-Rad N, Lytwyn M, Fang T, Kirkpatrick I, Jassal DS. Delayed contrast enhancement cardiac magnetic resonance imaging in trastuzumab induced cardiomyopathy. J Cardiovasc Magn Reson Off J Soc Cardiovasc Magn Reson. 2008;10:5.
104. Puntmann VO, Peker E, Chandrashekhar Y, Nagel E. T1 mapping in characterizing myocardial disease: a comprehensive review. Circ Res. 2016;119(2):277–99.
105. Taylor AJ, Salerno M, Dharmakumar R, Jerosch-Herold M. T1 mapping: basic techniques and clinical applications. JACC Cardiovasc Imaging. 2016;9(1):67–81.
106. Lurz P, Luecke C, Eitel I, Föhrenbach F, Frank C, Grothoff M, et al. Comprehensive cardiac magnetic resonance imaging in patients with suspected myocarditis: the MyoRacer-trial. J Am Coll Cardiol. 2016;67(15):1800–11.
107. Child N, Suna G, Dabir D, Yap M-L, Rogers T, Kathirgamanathan M, et al. Comparison of MOLLI, shMOLLLI, and SASHA in discrimination between health and disease and relationship with histologically derived collagen volume fraction. Eur Heart J Cardiovasc Imaging. 2018;19(7):768–76.
108. Hinojar R, Foote L, Arroyo Ucar E, Jackson T, Jabbour A, Yu C-Y, et al. Native T1 in discrimination of acute and convalescent stages in patients with clinical diagnosis of myocarditis: a proposed diagnostic algorithm using CMR. JACC Cardiovasc Imaging. 2015;8(1):37–46.
109. Winau L, Hinojar Baydes R, Braner A, Drott U, Burkhardt H, Sangle S, D'Cruz DP, Carr-White G, Marber M, Schnoes K, Arendt C, Klingel K, Vogl TJ, Zeiher AM, Nagel E, Puntmann VO. Ann Rheum Dis. 2018 Nov;77(11):1590-1598. High-sensitive troponin is associated with subclinical imaging biosignature of inflammatory cardiovascular involvement in systemic lupus erythematosus. Ann Rheum Dis. 2018 Nov;77(11):1590-1598.
110. Bohnen S, Radunski UK, Lund GK, Kandolf R, Stehning C, Schnackenburg B, et al. Performance of T1 and T2 mapping cardiovascular magnetic resonance to detect active myocarditis in patients with recent-onset heart failure. Circ Cardiovasc Imaging. 2015;8(6).
111. Puntmann VO, Carr-White G, Jabbour A, Yu CY, Gebker R, Kelle S, Rolf A, Zitzmann S, Peker E, D'Angelo T, Pathan F, Elen, Valbuena S, Hinojar R, Arendt C, Narula J, Herrmann E, Zeiher AM, Nagel E. Native T1 and ECV of Noninfarcted Myocardium and Outcome in Patients With Coronary Artery Disease. International T1 Multicentre CMR Outcome Study. J Am Coll Cardiol. 2018 Feb 20;71(7):766-778.
112. Farhad H, Staziaki PV, Addison D, Coelho-Filho OR, Shah RV, Mitchell RN, et al. Characterization of the changes in cardiac structure and function in mice treated with anthracyclines using serial cardiac magnetic resonance imaging. Circ Cardiovasc Imaging. 2016;9(12).
113. Moslehi JJ, Salem J-E, Sosman JA, Lebrun-Vignes B, Johnson DB. Increased reporting of fatal immune checkpoint inhibitor-associated myocarditis. Lancet. 2018;391(10124):933.
114. Mukai-Yatagai N, Haruki N, Kinugasa Y, Ohta Y, Ishibashi-Ueda H, Akasaka T, et al. Assessment of myocardial fibrosis using T1-mapping and extracellular volume measurement on cardiac magnetic resonance imaging for the diagnosis of radiation-induced cardiomyopathy. J Cardiol Cases. 2018;18(4):132–5.
115. Valbuena-López S, Hinojar R, Puntmann VO. Cardiovascular magnetic resonance in cardiology practice: a concise guide to image acquisition and clinical interpretation. Rev Espanola Cardiol Engl Ed. 2016;69(2):202–10.
116. Skitch A, Mital S, Mertens L, Liu P, Kantor P, Grosse-Wortmann L, et al. Novel approaches to the prediction, diagnosis and treatment of cardiac late effects in survivors of childhood cancer: a multi-centre observational study. BMC Cancer. 2017;17(1):519.
117. Heck SL, Gulati G, Hoffmann P, von Knobelsdorff-Brenkenhoff F, Storås TH, Ree AH, et al. Effect of candesartan and metoprolol on myocardial tissue composition during anthracycline treatment: the PRADA trial. Eur Heart J Cardiovasc Imaging 2017.